Electronic Supporting Information to Surface engineering of silica nanoparticles with a gadolinium-PCTA complex for efficient T_1-weighted MRI contrast agents.

Paul Mathieu[1, 2], Marie Chalet[3,4], Marie Myriam Clain[3,4], Lauryanne Teulon[1, 2], Eric Benoist[3,4], Nadine Leygue[3,4], Claude Picard[3,4], Sébastien Boutry[5,6], Sophie Laurent[5,6], Dimitri Stanicki[5], Céline Hénoumont[5], Fernando Novio[7], Julia Lorenzo[8], David Montpeyó[8], Diana Ciuculescu-Pradines,[1,2] Catherine Amiens[1, 2].

[1] CNRS, LCC (Laboratoire de Chimie de Coordination), 205 route de Narbonne, BP 44099, F-31077 Toulouse Cedex 4, France.
[2] Université de Toulouse, UPS, INPT, F-31077 Toulouse Cedex 4, France.
[3] CNRS, Laboratoire de Synthèse et Physico-Chimie de Molécules d'Intérêt Biologique (SPCMIB), UMR- 5068, 118 Route de Narbonne, 31062 Toulouse cedex 9, France.
[4] Université de Toulouse, UPS, Laboratoire de Synthèse et Physico-Chimie de Molécules d'Intérêt Biologique, SPCMIB, Toulouse, France.
[5] Department of General, Organic and Biomedical Chemistry, NMR and Molecular Imaging Laboratory, University of Mons, 19 avenue Maistriau, B- 7000 Mons, Belgium.
[6] Center for Microscopy and Molecular Imaging (CMMI), Université de Mons (UMONS), B-6041 Charleroi, Belgium
[7] Departament de Química, Universitat Autònoma de Barcelona (UAB), Campus UAB, 08193 Cerdanyola del Vallès, Barcelona, Spain
[8] Institut de Biotecnologia i Biomedicina, Departament de Bioquímica i de Biologia Molecular, Universitat Autònoma de Barcelona, 08193 Bellaterra, Spain.

1. List of abbreviations

1BR3G : Human transformed skin fibroblasts; AcOEt: ethyl acetate; Ag_2O: silver oxide; Al_2O_3 : alumina; APTMS: aminopropyl trimethoxysilane; ARM: atom resolved microscopy; ATR: attenuated total reflectance; $BrCH_2COOtBu$: tert-butyl bromoacetate; CA: contrast agent; $CaCl_2$: Calcium chloride; $CDCl_3$: Deuterochloroform; CH_2Cl_2: Dichloromethane; CH_3CN: Acetonitrile; -COOH: carboxylic acid function; DBPS : disinfection by-products; DHYD: hydrodynamic diameter; DIAD: Diisopropyl azodicarboxylate; DLS: dynamic light scattering; DMEM: Dulbecco's Modified Eagle Medium; DMF: dimethylformamide; DMSO: dimethylsulfoxide; DOTAGA: 2-(*R*)-2-(4,7,10-tris(carboxymethyl)-1,4,7,10-tetraazacyclododec -1-yl)pentanedioic acid ; DRIFT: Diffuse reflectance infrared Fourier transform; DTPA: diethylenetriaminepentaacetic acid; EDC: N-(3-Dimethylaminopropyl)-N'-ethylcarbodiimide hydrochloride; EDTA: ethylenediaminetetraacetic acid; EDX: energy dispersion X-Ray analysis; EtOH: ethanol; FT: Fourier Transform; HCl : hydrochloric acid; HCT116: Human colorectal carcinoma cells; HRMS(ESI) : electrospray high resolution mass spectrum; IC_{50}: median inhibitory concentration; ICP-OES: inductively coupled plasma-optical emission spectrometry ; Igepal-CO520: Polyoxyethylene (5) nonylphenylether, branched; IR: infrared; KI: potassium iodide; MCM-48: Mobil Composition of Matter N^{o}. 48 ; MeOH: methanol; MS (ESI): electrospray mass spectrum; $MgSO_4$: magnesium sulphate; MRI: magnetic resonance imaging; Na_2CO_3: sodium carbonate; $NaBH_4$: sodium tetraborohydride; $NaHCO_3$: sodium hydrogen carbonate; NaOH: sodium hydroxide; NBS: N-bromosuccinimide; NH_2: amino; NH_4OH: ammonia; NP nanoparticle; NMR: nuclear magnetic resonance; NMRD: nuclear magnetic relaxation dispersion; PBS: phosphate buffer solution; PCTA : Pyridine Containing TriAza; 3,6,9,15-tetraazabicyclo[9.3.1]pentadeca-1(15),11,13-triene-3,6,9-triacetic acid ; PDI: polydispersity index; PEG: polyethyleneglycol; PPh_3: triphenylphosphine, SBM: Solomon and Bloembergen model ; Si-DTTA: 3,6,9-Tris(carboxymethyl)-13,13-dimethoxyl-14-oxa-3,6,9-triaza-13-silaphentadecanoic acid ; SiO_2: silica; $-Si(OEt)_3$: triethoxysilyl; STEM-HAADF: scanning transmission electron microscopy-high angle annular dark field; sulfo-NHS: N-hydroxysulfosuccinimide sodium salt; TBDPSCl: tert-Butyl(chloro)diphenylsilane; tBu : tert-butyl; TEM: transmission electron microscopy; TESPIC: 3-(triethoxysilyl)propylisocyanate ; THF: tetrahydrofurane; TsCl: Tosyl chloride (toluene sulfonylchloride); ZP: zetapotential.

2. Pure silica NPs ($NPSiO_2$):

The synthesis of **$NPSiO_2$** was carried out following the procedure published in a previous publication[1]. Depending on the reaction time two sets of NPs could be obtained.

After 24h of reaction, a 10 mL dispersion of the NPs in milliQ water was obtained [$NPSiO_2$] ≅ 3.0 $mg.mL^{-1}$ (**solution 1**). Their average diameter was 25.9 ± 4 nm as determined after analyzing TEM images and their Z-average hydrodynamic diameter was 158 nm (PDI 15 %).

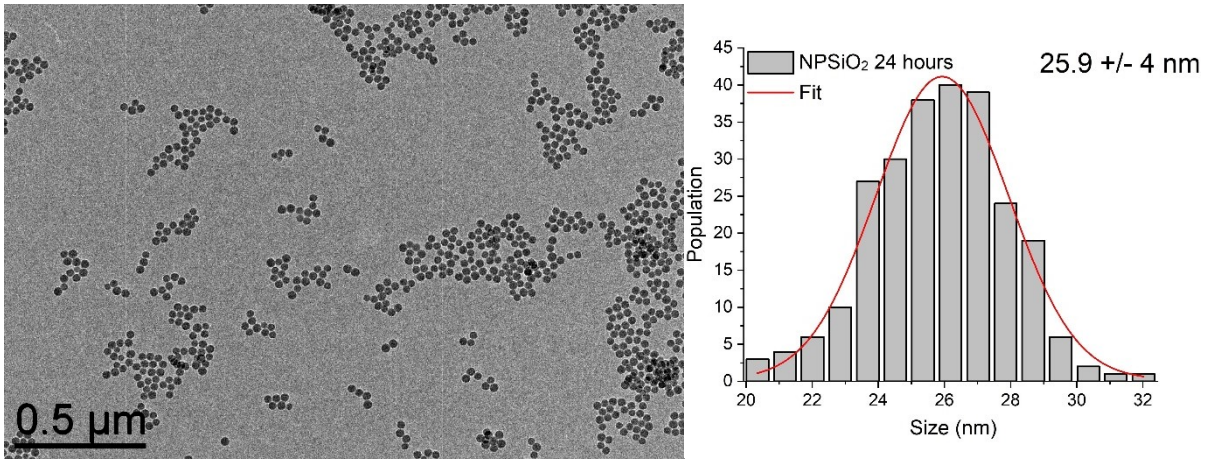

Figure ESI 1 : Typical TEM micrograph of **$NPSiO_2$** (24h) and corresponding size distribution

After 48h of reaction, a 10 mL dispersion of the NPs in milliQ water was obtained [$NPSiO_2$]≅ 2.5 mg.mL^{-1} (**solution 2**). Their average diameter was 23.2 ± 3.6 nm as determined after analyzing TEM images and their Z-average hydrodynamic diameter was 104 nm (PDI 16%).

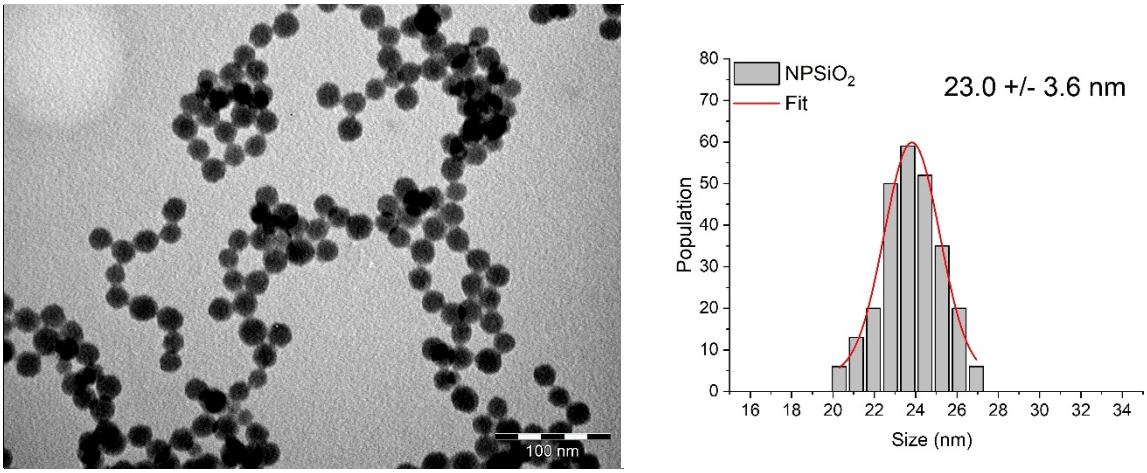

Figure ESI 2 : Typical TEM micrograph of **$NPSiO_2$** (48h) and corresponding size distribution

3. NH_2 modified silica NPs ($NPSiO_2$-NH_2) :

Surface functionalisation of **$NPSiO_2$** was carried out on a batch of **$NPSiO_2$** (24h, **solution 1** as described above), following a procedure described in [2]. Typically, 1.6 µL (9 µmol) of aminopropyltrimethoxysilane was added to the crude micellar solution which was then stirred for 5 minutes and left to react for 24 hours without supplementary stirring. The particles were washed by centrifugation twice with methanol, twice with ethanol and twice with milliQ water (centrifugation of 9000 rpm, 30 min., 5°C). Typically, a 10 mL dispersion of the NPs in milliQ water was obtained [$NPSiO_2$] ≅ 2.5 mg.mL^{-1}. The NPs displayed a grafting density of 2 N/nm² determined on the basis of CHN analysis among which 0.5 N/nm² are readily accessible (based on fluorescence titration using fluorescamine as NH_2 specific reagent [3]). Their average diameter was 24.6 ± 2.7 nm as determined after analyzing TEM images and their Z-average hydrodynamic diameter was 196 nm (PDI 24 %). Prior to the

amidic coupling, 4 batches of NPs were combined (alternatively the process could be scaled up without any change in the characteristics of the NPs), centrifugated and the NPs were washed once with PBS (10mM, pH=7.4), then redispersed in 15mL PBS (**solution 3**: around 100mg of **$NPSiO_2$-NH_2** corresponding to around 10 µmol of free NH_2 groups).

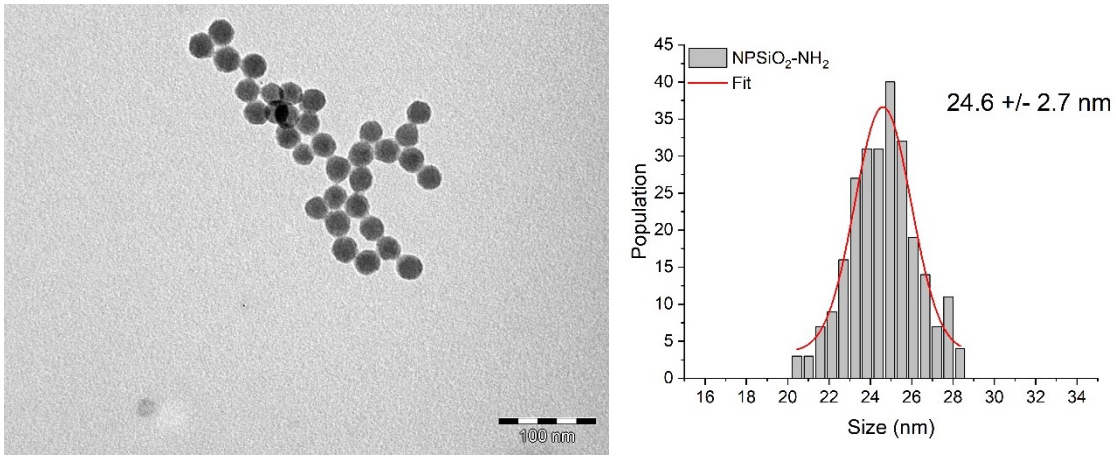

Figure ESI 3 : Typical TEM micrograph of **$NPSiO_2$-NH_2** and corresponding size distribution

4. ^{1}H et ^{13}C NMR ($CDCl_3$, 300 and 75MHz, respectively) of compounds 10 and 12

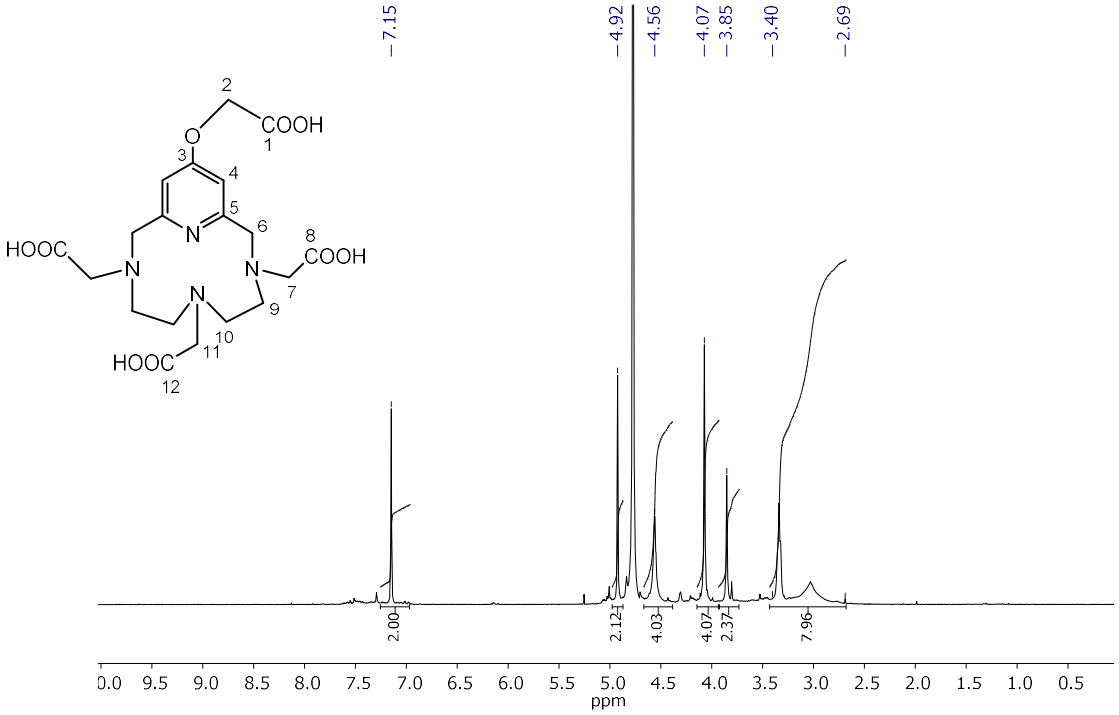

Figure ESI 4 : ^{1}H NMR spectrum (300 MHz, D_2O) of free ligand **10**. δ= 7.15 (s, 2H, 2CH, H_4), 4.92 (s, 2H, CH_2, H_2), 4.56 (s, 4H, $2CH_2$, H_6), 4.07 (s, 4H, CH_2, H_7), 3.85 (s, 2H, CH_2, H_{11}), 3.40-2.70 (m, 8H, $4CH_2$, H_9, H_{10}).

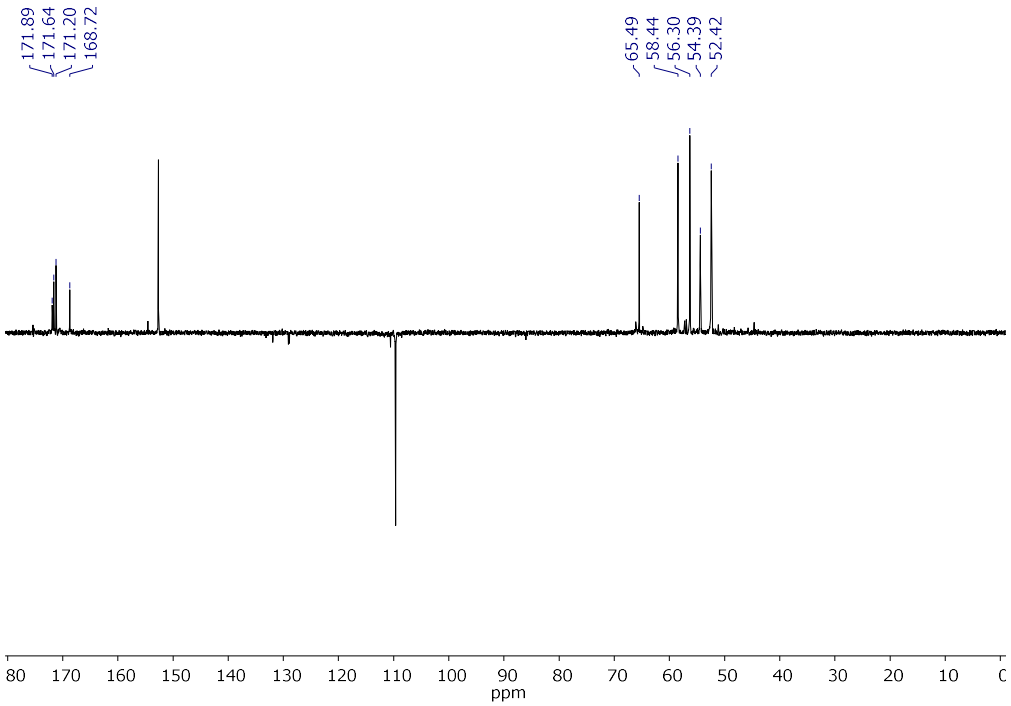

Figure ESI 5 : ^{13}C NMR spectrum (75 MHz, D_2O) of free ligand **10**: δ= 171.9 (Cq, C_{12}), 171.6 (Cq, C_8), 171.2 (Cq, C_1), 168.7 (Cq, C_3), 152.7 (Cq, C_5), 109.7 (CH, C_4), 65.6 (CH_2, C_2), 58.4 (CH_2, C_6), 56.3 (CH_2, C_7), 54.4 (CH_2, C_{11}), 52.42 (CH_2, C_9), 52.38 (CH_2, C_{10}).

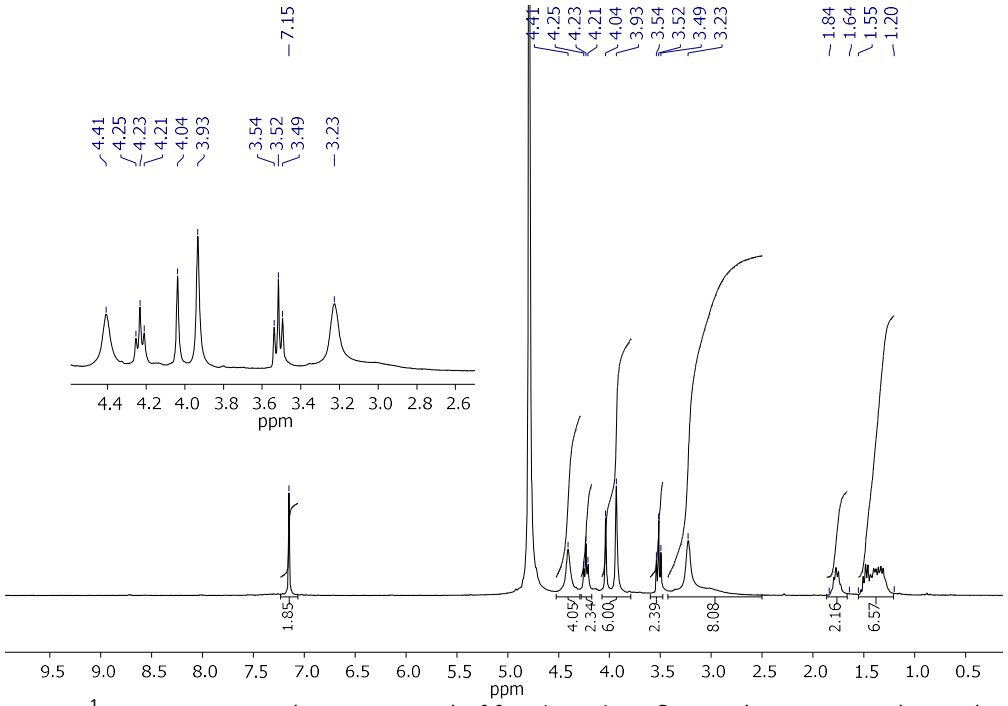

Figure ESI 6 : ^{1}H NMR spectrum (300 MHz, D_2O) of free ligand **12**: δ =7.15 (s, 2H, 2CH, H_8), 4.41 (s, 4H, $2CH_2$, H_{10}), 4.23 (t, J = 6.3 Hz, 2H, CH_2, H_6), 4.04 (s, 2H, CH_2, H_{15}), 3.93 (s, 4H, $2CH_2$, H_{11}), 3.52 (t, J = 6.5 Hz, 2H, CH_2, H_1), 3.23 (s, 8H, $4CH_2$, H_{13}, H_{14}), 1.81 – 1.73 (m, 2H, CH_2, H_5), 1.51 – 1.31 (m, 6H, $3CH_2$, H_2, H_3, H_4).

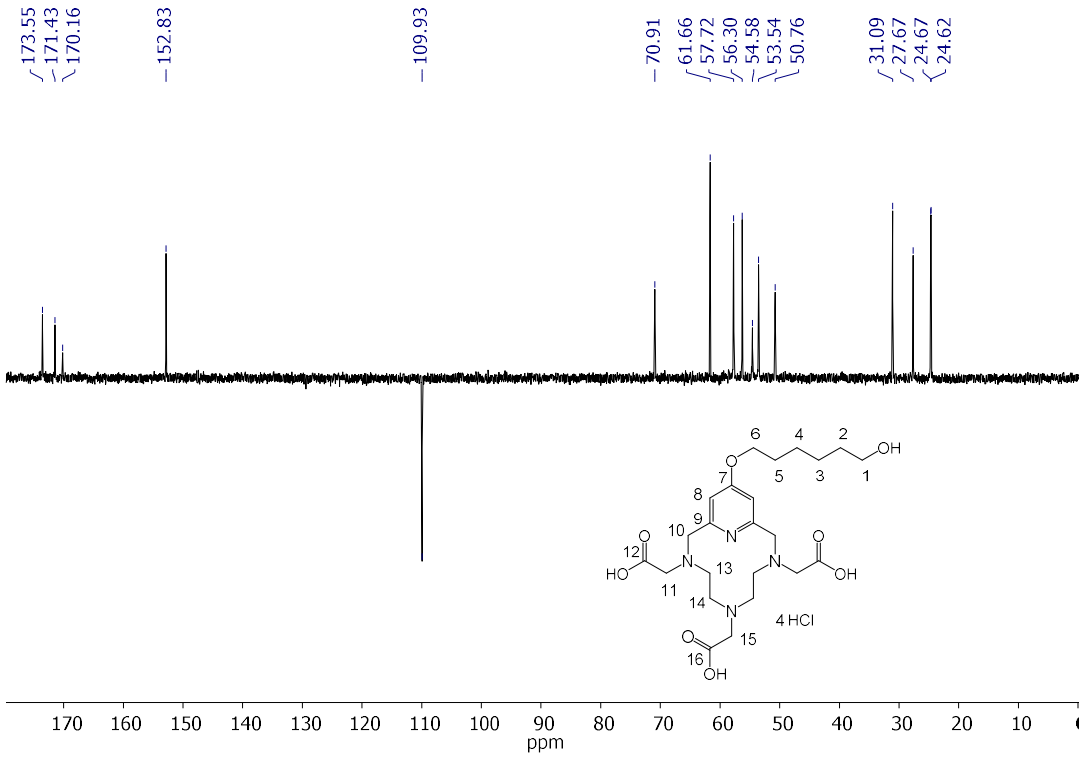

Figure ESI 7: ^{13}C NMR spectrum (75 MHz, D_2O) of free ligand **12**: δ= 173.5 (Cq, C_{12}), 171.4 (Cq, C_{16}), 170.2 (Cq, C_7), 152.8 (Cq, C_9), 109.9 (CH, C_8), 70.9 (CH_2, C_6), 61.7 (CH_2, C_1), 57.7 (CH_2, C_{10}), 56.3 (CH_2, C_{11}), 54.6 (CH_2, C_{15}), 53.5 (CH_2, C_{13}), 50.8 (CH_2, C_{14}), 31.1 (CH_2, C_2), 27.7 (CH_2, C_5), 24.7 (CH_2, C_3 or C_4), 24.6 (CH_2, C_3 or C_4).

5. HRMS (ESI$^+$) spectra of Gd-COOH anf Gd-OH

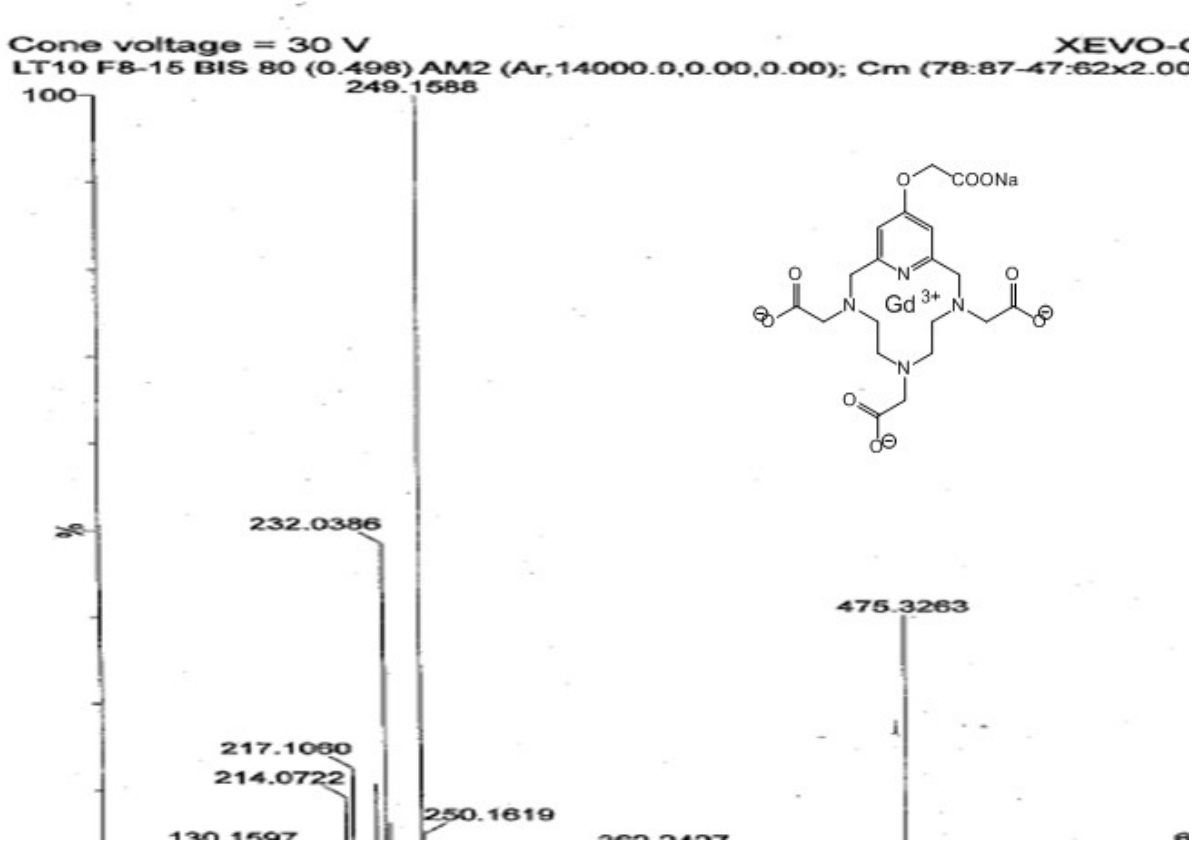

Figure ESI 8 : HRMS (ESI$^+$) spectrum of **Gd-COOH**.

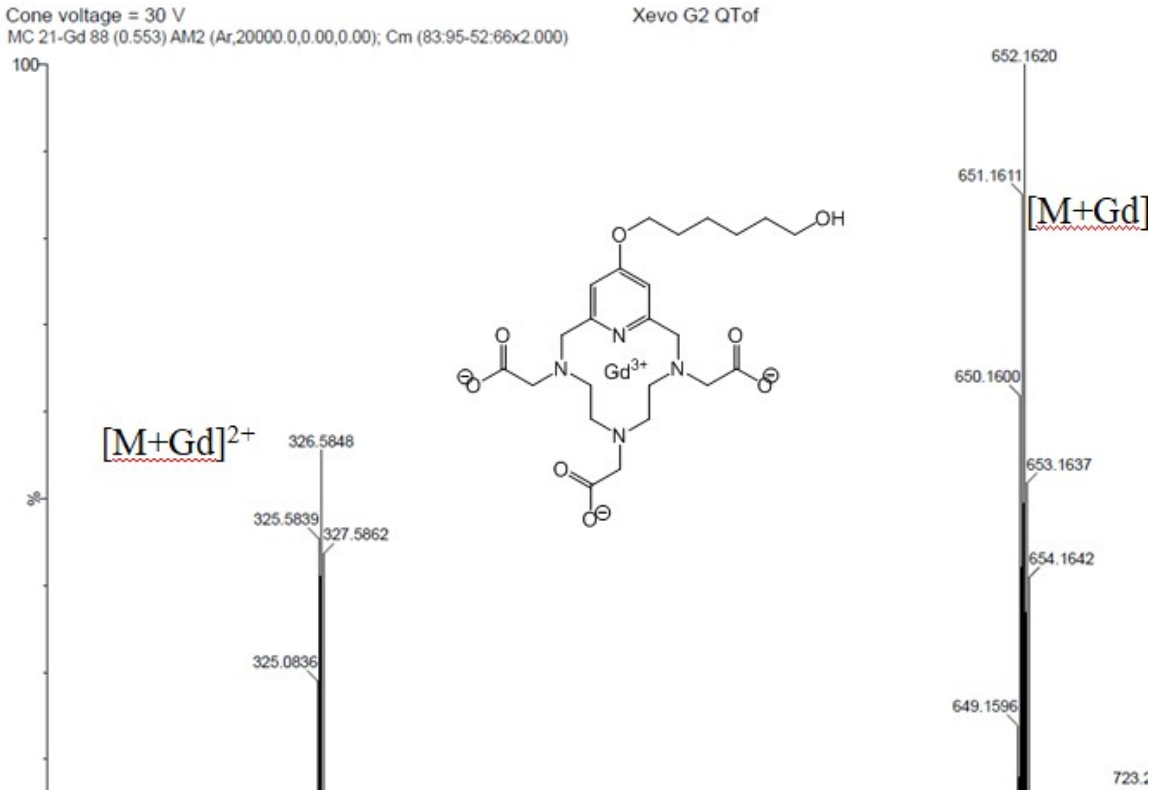

Figure ESI 9 : HRMS (ESI$^+$) spectrum of **Gd-OH**.

6. Amidic coupling of between $NPSiO_2$ and Gd-COOH

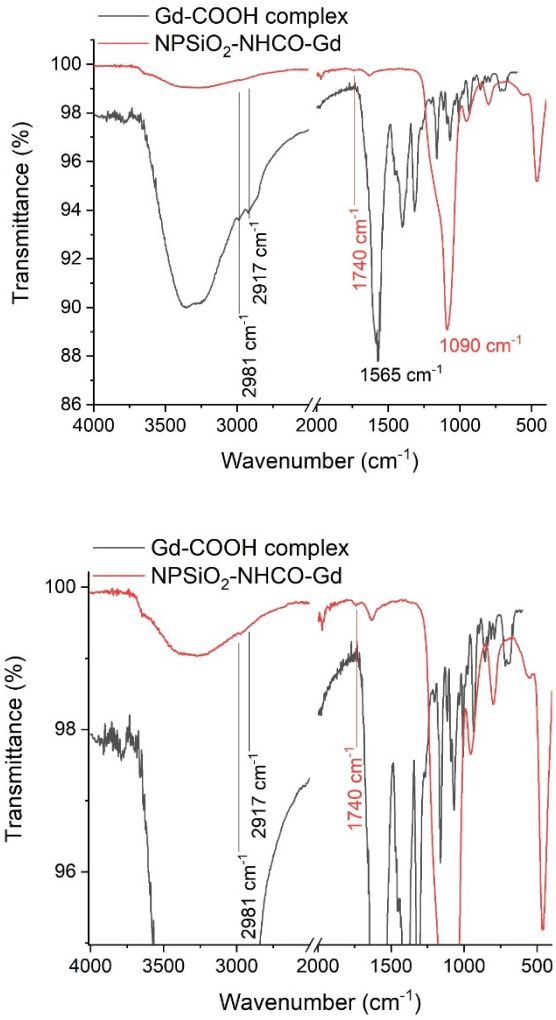

Figure ESI 10 : FT-IR (ATR mode) of **Gd-COOH** and of **$NPSiO_2$-NHCO-Gd**. Top : full scale ; bottom : enlargement along the y axis to emphasize the weak contribution of the amide bond.

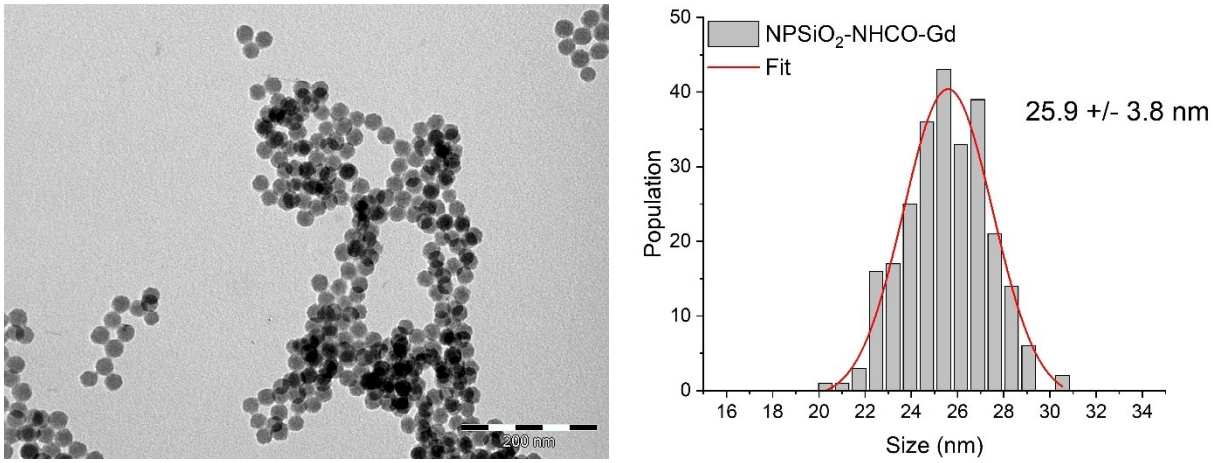

Figure ESI 11 : Typical TEM micrograph of **$NPSiO_2$-NHCO-Gd** and corresponding size distribution (scale bar: 200 nm) and corresponding size distribution

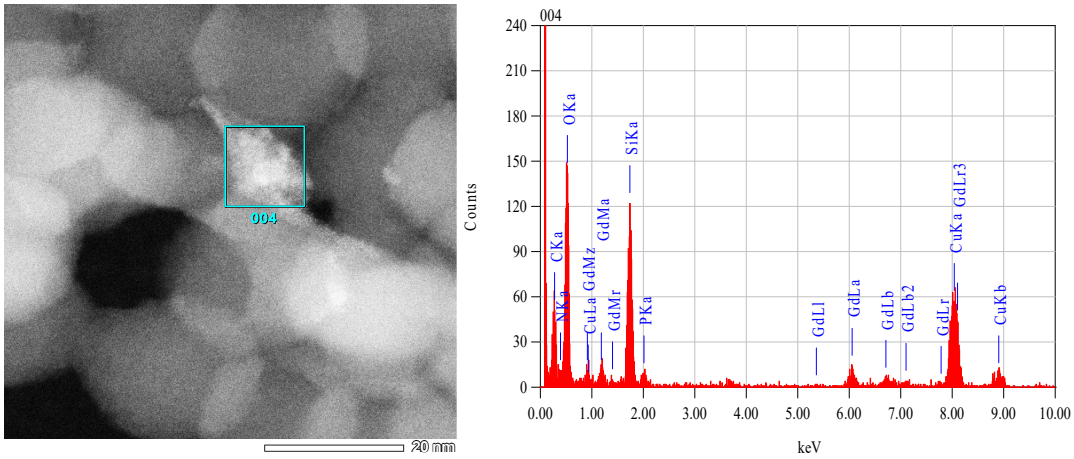

Figure ESI 12: left: ARM image of the nanomaterial (scale bar: 20nm), and right: EDX analyses corresponding to the region delineated by the square in the left image.

7. Condensation between $NPSiO_2$ and Gd-Si(OEt)$_3$

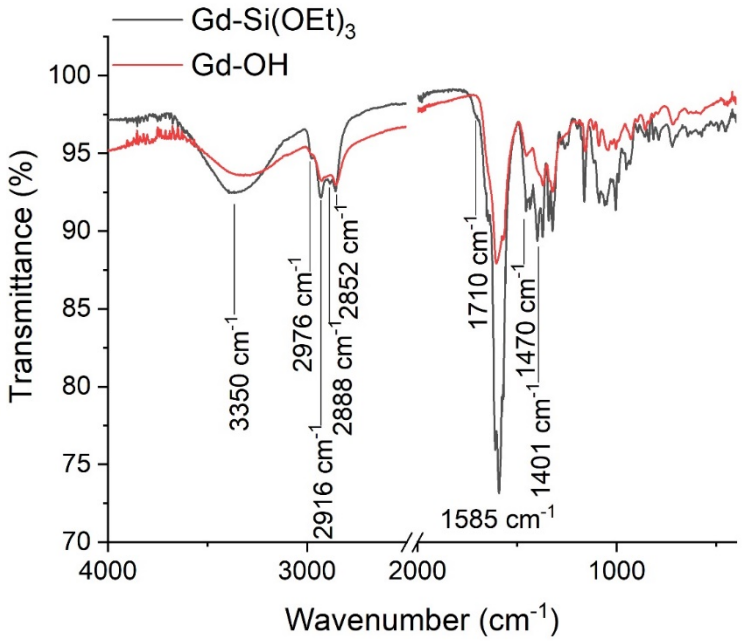

Figure ESI 13: FT-IR (ATR mode) of **Gd-Si(OEt)$_3$** and of **Gd-OH**. Due to the presence of two water molecules in the complexe, a hump is still observed in the OH region but its relative intensity is much lower than in the **Gd-OH** complex in agreement with the formation of the urethane bond.

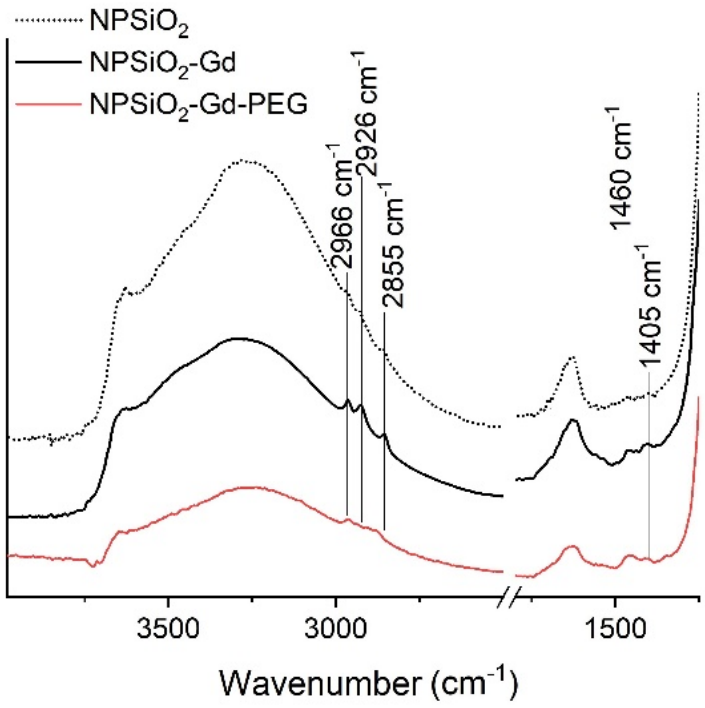

Figure ESI 14: DRIFT spectra of **$NPSiO_2$**, **$NPSiO_2$-Gd** and **$NPSiO_2$-Gd-PEG**

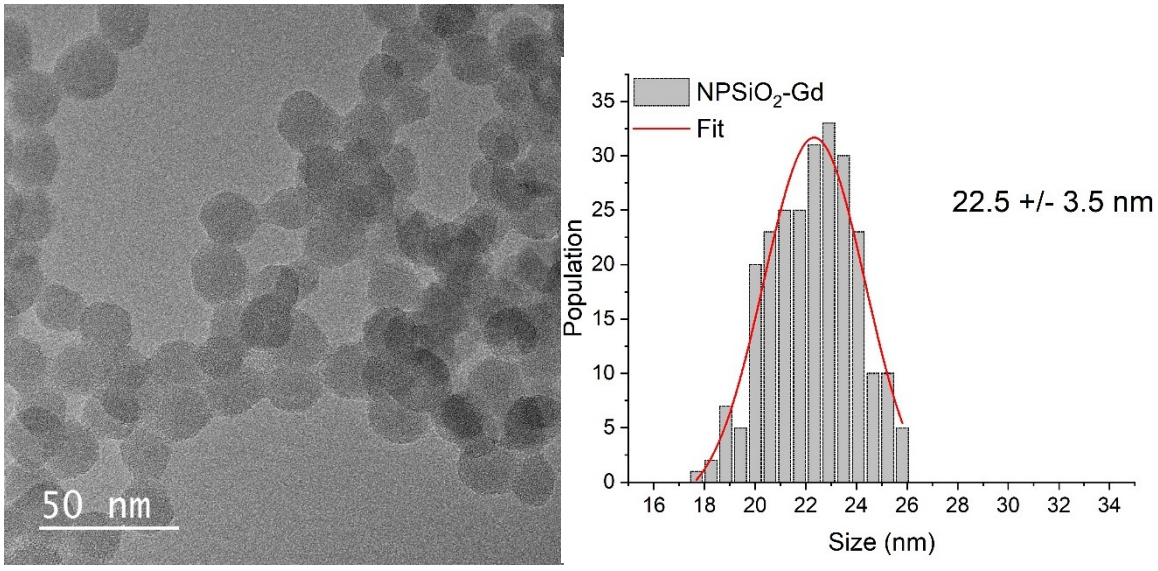

Figure ESI 15 : Typical TEM micrograph of **$NPSiO_2$-Gd** and corresponding size distribution

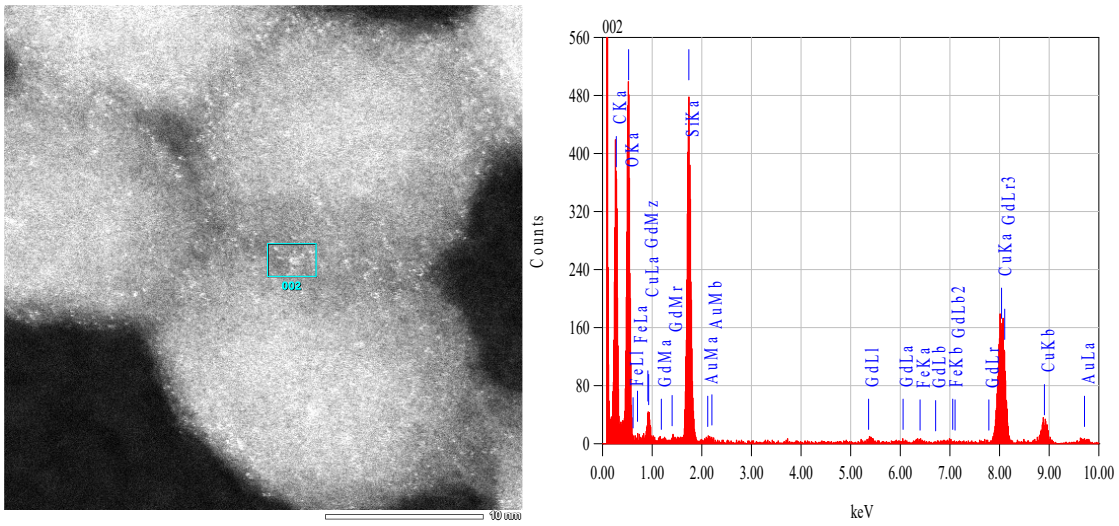

Figure ESI 16 : ARM image of **$NPSiO_2$-Gd** (left, scale bar : 10nm) and EDX analysis (right) of a region presenting a high concentration of heavy atoms (the weak Fe signal arises from the polar parts of the microscope, Cu, Au, C and O ones from the grid). This region is delineated by a square in the left image.

8. Complementary data on cytotoxicity

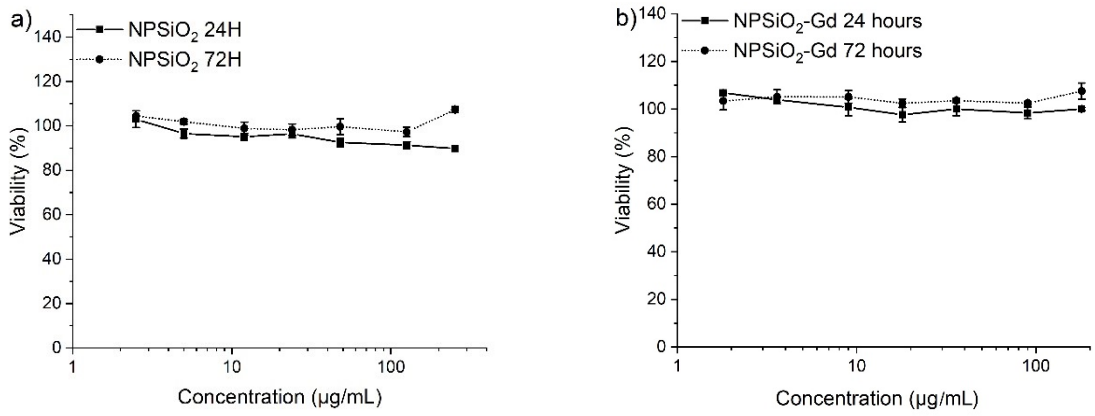

Figure ESI 17 : Cytotoxicity studies (viability versus concentration) of a) **$NPSiO_2$** and b) **$NPSiO_2$-Gd** ([$NPSiO_2$-Gd]= 1µg/mL <=> [Gd]= 0.4 µmol/L)

References

1 P. Mathieu, Y. Coppel, M. Respaud, T. Q. Nguyen, S. Boutry, S. Laurent, D. Stanicki, C. Henoumont, F. Novio, J. Lorenzo, D. Montpeyó and C. Amiens, *Molecules*, 2019, **24**, 4629.

2 C. Tissandier, N. Diop, M. Martini, S. Roux, O. Tillement and T. Hamaide, *Langmuir*, 2012, **28**, 209–218.

3 O. Makrygenni, E. Secret, A. Michel, D. Brouri, V. Dupuis, A. Proust, J.-M. Siaugue and R. Villanneau, *J. Colloid Interface Sci.*, 2018, **514**, 49–58.